Investigating Time-Varying Brain Connectivity with Functional Magnetic Resonance Imaging using Sequential Monte Carlo

Pierfrancesco Ambrosi[1], Mauro Costagli[2,3], Ercan E Kuruoğlu[4],
Laura Biagi[3,2], Guido Buonincontri[3,2], Michela Tosetti[3,2]

[1] Department of Physics, University of Pisa, Pisa, Italy (pfa2804@gmail.com)
[2] Imago 7 Research Center, Pisa, Italy (mcostagli@imago7.eu)
[3] Laboratory of Medical Physics and Magnetic Resonance, IRCCS Stella Maris, Pisa, Italy
(laura.biagi@fsm.unipi.it, guido.buonincontri@fsm.unipi.it, michela.tosetti@fsm.unipi.it)
[4] Institute of Information Science and Technologies, CNR, Pisa, Italy (ercan.kuruoglu@isti.cnr.it)

***Abstract*—There is a rising interest in studying the degree of connection and the causal relationships between brain regions, as a growing body of evidence suggests that features of these interactions could play a role as markers in a host of neurological diseases. The vast majority of brain connectivity studies treats the brain network as stationary. New insights on the temporal behaviour of these connections could significantly improve our understanding of brain networking in both physiology and pathology. In this paper, we propose the application of a computational methodology, named Particle Filter (PF), to functional Magnetic Resonance Imaging (fMRI) data. The PF algorithm aims to estimate time-varying hidden variables of a given observational model through a Sequential Monte Carlo approach. The fMRI data are represented as a first-order linear time-varying Vector Autoregression model (VAR). On simulated time series, the PF approach effectively detected and enabled to follow time-varying hidden parameters and it captured causal relationships among signals. The method was also applied to real fMRI data and provided similar results to those obtained by using a different proxy measure of causal dependency, that is, correlation between delayed time series. Interestingly, the PF approach also enabled to detect statistically significant changes in the cause-effect relationships between areas, which correlated with the underlying stimulation pattern delivered to subjects during the fMRI acquisition.**

***Index Terms*—brain connectivity, fMRI, sequential Monte Carlo, Particle Filtering, VAR model**

I. Introduction

To improve our understanding of brain functioning, it is crucial to study the dynamic interplay among anatomically segregated and functionally distinct brain areas.

While structural connectivity describes the anatomical connection between brain regions, functional and effective connectivity refer to two different ways to quantify the interaction among brain regions [1].

Functional connectivity describes connections between brain regions in terms of statistical codependency: it is non-directional and model-free [2]. On the contrary, effective connectivity describes the temporal relationship and causal influence between brain regions included in a defined network model [3].

Functional magnetic resonance imaging (fMRI) enables to implement, in a non-invasive manner and with satisfactory spatiotemporal resolution, all these complementary approaches to study brain connectivity, in both physiology and pathology, such as in Alzheimer's disease [4]–[6], schizophrenia [7] and Major Depression Disorder [8].

It has been proposed that brain dynamics, and in particular effective connectivity, may constitute a biological marker for specific brain diseases and could be used to monitor response to treatment [9]–[12]. The most widespread methods to investigate effective connectivity are Granger Causality (GC) and Dynamic Causal Modeling (DCM). GC is based on the principle that if the knowledge of the temporal evolution of a given brain region A improves the predictability of the temporal evolution of another brain region B, A is said to Granger-cause B [13]–[15]. Since this approach is based on the evaluation of a linear codependence between time series, it is limited by the assumption of stationarity in the coupling between regions or by the need to employ a sliding-window approach to address temporal variations. Differently, DCM relies on the the use of a model describing the predicted relationship between neural activity and observed fMRI signal [16].

A different, promising approach to investigate time-varying brain connectivity is the Sequential Monte Carlo (SMC) methodology [17], [18]. SMC approaches aim to estimate the internal, hidden states in dynamic systems when only partial and noisy observations are available.

A specific SMC methodology which employs discrete majors to approximate density functions and updates the posteriors with the arrival of each new sample using sequential importance sampling is called Particle Filtering (PF).

Ahmad et al. [19] adopted a symmetric, linear, first-order, time-varying auto-regressive (TVAR) model and used PF to estimate the temporal relationships among fMRI time-series

representing four brain regions during resting state. The symmetric nature of their model enabled the use of a small set of free parameters, which allowed them to achieve a satisfactory description of the time-varying statistical relationship among brain regions; however, it prevented the estimation of the directional cause/effect dependencies, that is, their approach cannot be used to investigate effective connectivity.

The backbone of the model and algorithm proposed in our study is the recent SMC approach by Ancherbak et al. [20], originally developed for time-varying gene network modelling, which we adapted for studying brain connectivity by using fMRI data. The feasibility and behaviour of the proposed approach has been studied on synthetic data mimicking fMRI time-series. The method was also applied to real fMRI datasets. Results were compared to a proxy measure of effective connectivity, that is, delayed correlation.

II. Methodology

A. Model and algorithm

Particle filtering [20]–[23] is a sequential Monte Carlo methodology based on the Bayes theorem on conditional probability. Particle filters estimate the probability distributions of hidden variables of interest, modelled according to a hypothesized *state-space equation*. Such probability distributions are estimated from the data, modelled according to a hypothesized *observation equation*. The probability density function (*pdf*) is allowed to be time-varying and is therefore sequentially updated when new data become available. In brain connectivity studies based on fMRI data, the relationship among the time-series of R different brain regions $\mathbf{x}$ can be modelled as a first order linear Vector AutoRegression (VAR) model [14], [23]–[26] as:

$$x_i(t) = \sum_{j}^{R} a_{ij}(t) x_j(t-1) + \eta_i(t) \qquad i = 1, \cdots, R \quad (1)$$

or in matrix notation:

$$\mathbf{x}_t = \mathbf{a}_t \mathbf{x}_{t-1} + \eta_t \quad (2)$$

which is employed as the observation equation describing the relationship between the observations $\mathbf{x}_t$ at time t and those at time $t-1$ (that is, $\mathbf{x}_{t-1}$); η_t is the observation noise; the hidden parameters of interest $\mathbf{a}_t$ represent the causal influence exerted between different areas. In particular, it can be assumed that $\mathbf{a}_t$ are allowed to be time-varying:

$$a_{ij}(t) = a_{ij}(t-1) + \nu_{ij}(t) \quad (3)$$

where $a_{ij}(t)$ is the ij-th element of the coefficients matrix $\mathbf{a}_t$, describing the influence of the j-th region over the i-th region, and $\nu_{ij}(t)$ is the process noise (innovation) term.

The PF algorithm evolves from an initial probability distribution for $a_{ij}(t-1)$, which we chose to be uniform, and through equation (3) it generates new possible values for $a_{ij}(t)$; then, with equation (2), the PF algorithm generates predicted values of the observations at time t. The desired probability density function of the parameters of interest $\mathbf{a}_t$ can be estimated via Bayes theorem as follows:

$$p(\mathbf{a}_t|\mathbf{x}_{1:t}) = \frac{p(\mathbf{x}_t|\mathbf{a}_t)p(\mathbf{a}_t|\mathbf{x}_{1:t-1})}{p(\mathbf{x}_t|\mathbf{x}_{1:t-1})} \quad (4)$$

and with the assumption of Gaussian noise we have

$$p(x_t|a_t) = \frac{1}{(2\pi\sigma_\eta^2)^{R/2}} \exp\Big(- \frac{(x_t - \hat{x}_t)^2}{2\sigma_\eta^2} \Big) \quad (5)$$

where $\hat{x}_t$ are the data estimated through (1) at time t. In most applications, (4) cannot be solved analytically [27], but it can be computed through the Sequential Monte Carlo sampling scheme, which consists in representing the pdf $p(\mathbf{a}_t|\mathbf{x}_{1:t})$ as a discrete set of N weighted samples called *particles*:

$$p(\mathbf{a}_t|\mathbf{x}_{1:t}) \approx \sum_{n=1}^{N} w_t^{(n)} \delta(\mathbf{a}_t - \mathbf{a}_t^{(n)}) \quad (6)$$

where $w_t^{(n)}$ are the weights associated to the n^{th} particle $\mathbf{a}_t^{(n)}$. The Sequential importance Sampling (SIS) [27] methodology provides a strategy to compute the weights. It can be shown [22] that the weights can be sequentially updated as follows:

$$w_t^{(n)} \propto w_{t-1}^{(n)} \cdot p(\mathbf{x}_t|\mathbf{a}_t) \quad (7)$$

where the proportionality takes into account normalization factors. With this approach, at each time instant t we have a sample set $\{\mathbf{a}_t^{(n)}, w_t^{(n)}\}$ for $n = 1, \ldots, N$ which can be used to estimate the pdf of the parameters and to infer information about the network. However, sequential Monte Carlo methodologies suffer from a problem called degeneracy: after some iterations, most of the particles will have a very low statistical weight, resulting in a lower exploration efficiency of the algorithm. To overcome this problem a step called resampling is performed at each time instant: if the number of effective particles, introduced in [28] as

$$N_{eff} = \frac{1}{\sum_{n=1}^{N} (w_t^{(n)})^2}$$

is below a certain arbitrary threshold, particles with low weight are substituted by copies of particles with high weight, resulting in a more effective exploration of the solution space.

The resulting algorithm can be schematically expressed as

- Input the BOLD fMRI data series $\mathbf{x}_t$
- Initialize the parameters and $\mathbf{a}_{t=0} = 0$
- for t=1:T
  - generate N particles from previous coefficients' values through (3) (updating step)
  - predict the values of the observations at time t from values at time $t-1$ with (2)
  - compute the likelihood between predicted values and observed values with (5)
  - normalize the weights and resample
- end for on t

This procedure is repeated N_r times, all independent from each other, to provide a better exploration of the solution

space. The final outputs of the algorithm are the $\mathbf{a}_t$ computed as the average of the N_r repetitions. The algorithm was implemented in MATLAB (Mathworks, Natick, MA, U.S.A.) R2017b.

B. Synthetic data

To validate the proposed approach, two different synthetic brain networks were used.

- One network with R=6 nodes, each with T=100 time points, stationary coefficients generated with the MATLAB function *VARM* with a Signal-to-Noise (SNR) ratio set to either ∞ ($\sigma_\eta = 0$, ideal case) or 6 dB (worst-case scenario). To demonstrate that the proposed approach reliably reflects the causal relationship between time series, we computed the Pearson's coefficients of linear correlation between the a_{ij} coefficients estimated by PF and the coefficients used to generate the synthetic data.
- Another network with R=2 and T=250 was used to assess the PF capability to capture time-varying hidden parameters. In this case, a_{ij} coefficients were zero except for coefficient a_{21}, whose value switched from 1 to -1 every 125 time points. The SNR was 10dB.

C. Real fMRI data

The proposed approach was also retrospectively applied to real fMRI data acquired on two healthy volunteers. Time-series consisted of 240 time points with a temporal resolution of 2 s, acquired at isotropic spatial resolution of $(1.5\ \text{mm})^3$ on a 7T MRI system. During acquisition, the subjects' thumb- and index-fingertips were stimulated via a pneumatic device (Linari Engineering, Pisa, Italy). The subjects' task was to

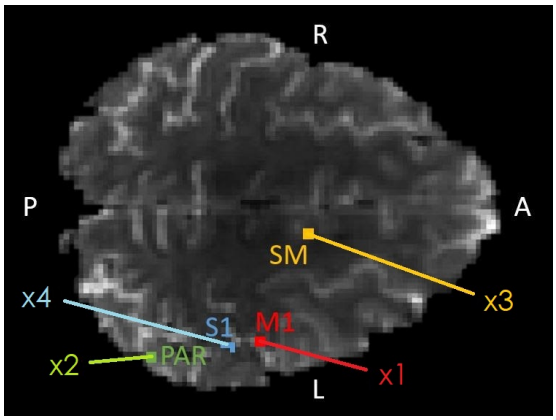

Figure 1. ROIs drawn on one representative subject, representing primary somatosensory (S1), primary motor (M1), supplementary motor (SM) and parietal (PAR) cortices. A, P, L, R indicate Anterior, Posterior, Left and Right sides of the brain.

move the stimulated fingers whenever they were stimulated. Networks of four nodes were studied: nodes consisted of voxels in Regions-of-Interest (ROIs) covering primary somatosensory (S1), primary motor (M1), supplementary motor (SM) and parietal (PAR) cortices. ROIs were manually drawn on each subject on one slice only, to avoid potential slice timing confounds (Fig. 1). The optimal order of the autoregressive model describing the time series was 1, as estimated by the Schwartz criterion [14]. In these fMRI datasets, the a_{ij} coefficients estimated by particle filtering were compared to the delayed correlation c_{ij} between signals $x_{i,t}$ and $x_{j,t-1}$ which reflect the time-invariant causal influence exerted by node j over node i.

III. Experimental Results and Discussions

A. Synthetic Data

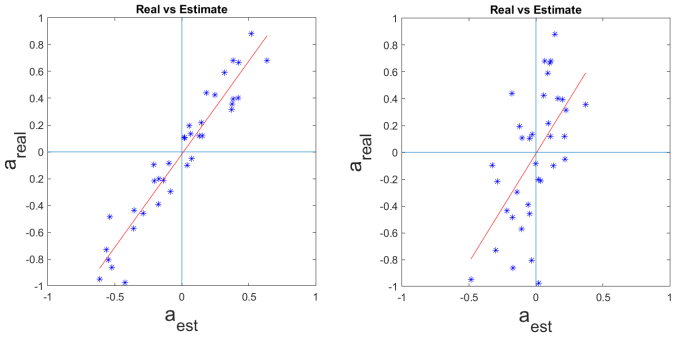

Figure 2. Scatter plots that relate PF estimates (x axis) and true values (y axis) of the auto-regressive model for a six-node network with 100 time samples, in the absence of noise (left) and with an additive noise (right) with SNR = 6 dB. The red lines are the results of a linear fit of the data: in the noiseless case the slope m and the offset q were 1.39 and $-1.62 \cdot 10^{-2}$, respectively; in the noisy case, m = 1.62 and q = $8 \cdot 10^{-3}$.

Scatter plots in Fig. 2 demonstrate that the causality coefficients estimated by PF in a stationary network satisfactorily correlate with the true coefficients, both in the noiseless synthetic dataset (Pearson's $\rho = 0.96$) and in the noisy scenario with SNR = 6 dB (Pearsons' $\rho = 0.59$).

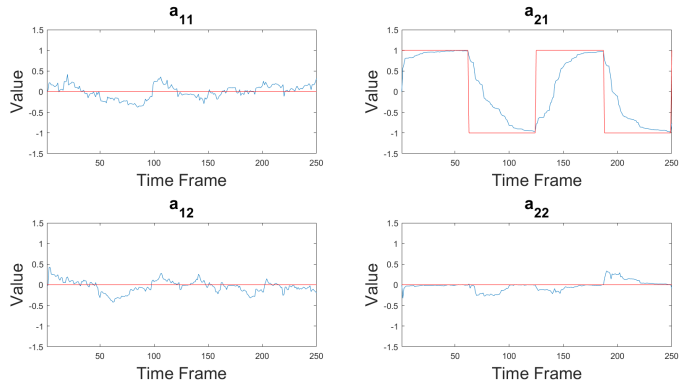

Figure 3. Time courses of the hidden parameters a_{ij} in the case of a 2-node network with non-stationary coefficient a_{21} alternating between 1 and -1. Red lines represent the true values, while blue lines represent the estimates obtained by PF.

The case of a network with one time-varying coefficient is shown in Fig. 3. The PF tracks the changes of the non-stationary coefficient a_{21}, although the estimated values do not immediately follow the abrupt changes between 1 and -1

and viceversa. All the other coefficients are correctly estimated to be close to the nominal null value.

B. Real fMRI Data

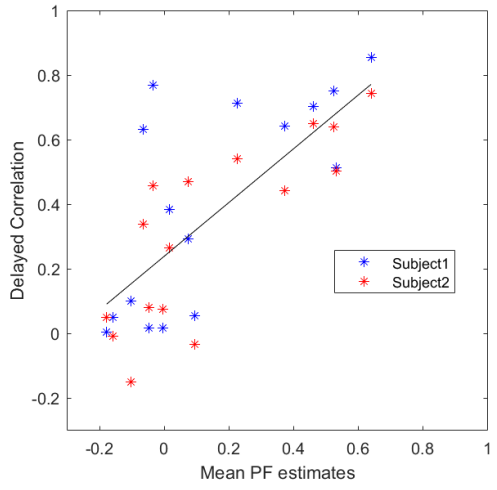

Figure 4. Scatter plot showing the relationship between mean PF estimates (horizontal axis) and delayed correlation (vertical axis) on two sets of real data. The Pearson's correlation coefficient is 0.74, which corresponds to a statistically significant correlation with $p < 0.001$. Slope and offset of the linear fit were 0.83 and 0.24 respectively.

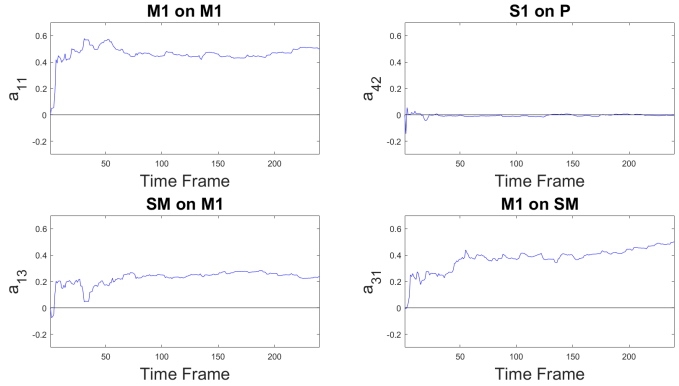

Figure 5. Plots in blue color show the PF-estimated time courses of four representative hidden parameters a_{ij} in the case of a 4-node network, estimated in real fMRI data in one subject. Top left panel depicts the coefficient representing the influence of time point t over time point $t-1$ within the primary motor area M1. Top right panel depicts the coefficient describing the negligible causal effect exerted by the primary somatosensory area S1 over the parietal cortex. Bottom panels represent the causal effect exerted by the Supplementary Motor area SM over M1 and viceversa.

The PF captured causal interactions between brain areas, which significantly correlated with a proxy measure of effective connectivity, that is, delayed correlation ($p < 0.001$, Pearson's correlation coefficient $\rho = 0.74$, Fig. 4). In particular, in both subjects, the highest a_{ij} coefficients in both PF and delayed correlation were those which represent the causal influence exerted by the primary motor and somatosensory areas, in agreement with current knowledge of brain functioning during a sensory-motor task. Fig. 5 exemplifies the brain connectivity temporal evolution through four representative a_{ij} coefficients in Subject 2: the top left panel depicts the coefficient representing the influence of area M1 at time $t-1$ over itself at time t. Crucially, this coefficient also exhibits statistically significant oscillations (t-test between coefficient values depending on the presence or absence of the sensorymotor task, $p < 0.05$) that vary with the same timing of the sensory-motor task. The top right panel displays one representative coefficient involving the parietal cortex, which is approximately 0 in accordance with the predictable non-involvement of this area in the task used here. Last, the two bottom panels demonstrate the expected reciprocal influence between M1 and SM areas.

Other studies previously proposed to apply SMC methods to fMRI data. Murray and Storkey [29] proposed a forward-backward Particle Filter using, as observation equation, a stochastic extension of the balloon model, which was proposed by Buxton et al. [30] to describe the haemodynamics that follow brain activity. In their study, the hidden parameters of the model resulted approximately constant, probably as a consequence to the complexity of the model itself. In a different study by Ahmad et al. [31] a Gibbs sampler in a VAR model with stationary coefficients was applied to fMRI data acquired during periodic visual stimulation alternating between on and off periods. The time series were artificially cut and recombined in order to form separate time series representing either the rest or the stimulated condition. The hidden model parameters of the network were found to be different between the two cases, however each time course representing each condition were considered stationary. The same group also described the use of a symmetric VAR model and a Rao-Blackwellized Particle Filter to study fMRI data acquired during resting state [19]. This assumption allowed to reduce the model complexity, because in the case of a symmetric model the number of degrees of freedom for R regions decreases from R^2 to $R(R-1)/2$ for every time point t, however this approach did not permit to infer neither the directionality of the network nor any possibly asymmetric cause/effect interaction between brain areas. The variations through time of the estimated coefficients were interpreted as actual variations in brain connectivity, however these results were not validated with different analyses.

Our implementation of the PF algorithm enabled to retrieve the hidden parameters in synthetic data mimicking a real network of fMRI time series. In particular, a convincing agreement with ground truth was demonstrated in the stationary case, and in the non-stationary case the estimated coefficients followed the time-varying hidden variables. In real fMRI data, the time-averaged PF estimates were in agreement with a proxy measure of causality, that is, delayed correlation. Part of the mismatch between the proposed method and delayed correlation could be explained by the fact that the PF algorithm studies the network as a whole and produces estimates of a_{ij} coefficients that update at every time instant,

while delayed correlation is a measure of pair-wise causality that does not take into account possible non-stationarities and spurious cause-effect relationships mediated by other nodes of the network.

IV. Conclusions

We utilized Particle Filtering to test and identify the time-varying brain connectivity as evidenced in fMRI images. Our experiments confirmed the hypothesis of time-varying brain connectivity pattern and gave evidence for non-symmetric connectivity. To the best of our knowledge, this is the first time that it was possible to detect, with a PF approach, statistically significant changes in cortical cause-effect relationships correlated with the underlying task-rest pattern during the fMRI acquisition.

Future studies should test the performance of the proposed algorithm in fMRI experiments with higher time resolution, possibly < 1 s, and they should aim to unveil possibly asymmetric changes in effective connectivity among brain regions. Also, to minimise the impact of vascular dynamics and highlight neural ones, future studies should use more sophisticated experimental designs that enable a better control over the non-uniformity of brain haemodynamics across different areas [32]–[34].

References

[1] K.J. Friston, "Functional and Effective Connectivity: a review," Brain Connectivity, vol. 1, pp. 13–36, 2011.

[2] A.M. Aertsen, G.L. Gerstein, M.K. Habib, G. Palm, "Dynamics of neuronal firing correlation: modulation of effective connectivity," Journal of Neurophysiology, vol. 61(5), 900-917, June 1989.

[3] K.E. Stephan, K.J. Friston, "Analyzing effective connectivity with functional magnetic resonance imaging," WIREs Cognitive Science, vol. 1, 446-459, 2010.

[4] M.D. Greicius, G. Srivastava, A.L. Reiss, V. Menon, "Default mode network activity distinguishes Alzheimer's disease from healthy aging: evidence from functional MRI," Proceedings of the Nationall Academy of Science of the USA, vol. 101, 4637-4642, 2004.

[5] M.D. Greicius, "Resting-state functional connectivity in neuropsychiatric disorders," Current Opinion in Neurology, vol. 21, 424-430, 2008.

[6] D.T. Jones, P. Vemuri, M.C. Murphy, J.L. Gunter, M.L. Senjem, M.M. Machulda et al., "Non-stationarity in the "resting brain's" modular architecture," PLoS One 7, e39731, 2012.

[7] M.P. van den Heuvel, "Exploring the brain network: A review on resting-state fMRI functional connectivity," European Neuropsychopharmacology, vol. 20, 519-534, 2010.

[8] M.D. Greicius, B.H. Flores, V. Menon, G.H. Glover, H.B. Solvason, H. Kenna et al., "Resting-state functional connectivity in major depression: abnormally increased contributions from subgenual cingulate cortex and thalamus," Biological Psychiatry, vol. 62, 429-437, 2007.

[9] V. Jirsa, A.R. McIntosh, "Handbook of Brain Connectivity," Berlin: Springer, 2007.

[10] G. Honey, E. Bullmore, "Human pharmacological MRI," Trends in Pharmacological Sciences, vol. 25, 366–374, 2004.

[11] K.E. Stephan, L.M. Harrison, W.D. Penny, K.J. Friston, "Biophysical models of fMRI responses," Current Opinion in Neurobiology, vol. 14, 629–635, 2004.

[12] I.I. Gottesman, T.D. Gould, "The endophenotype concept in psychiatry: etymology and strategic intentions," American Journal of Psychiatry, vol. 160, 636–645, 2003.

[13] R. Goebel, A. Roebroeck, D.-S. Kim, E. Formisano, "Investigating directed cortical interactions in time-resolved fMRI data using vector autoregressive modeling and Granger causality mapping", Magnetic Resonance Imaging, 21, 1251–1261, 2003.

[14] A. Roebroeck, E. Formisano, R. Goebel, "Mapping directed influence over the brain using Granger causality and fMRI," Neuroimage, 25, 230-42, 2005.

[15] G. Desphande, K. Sathian, X. Hu, "Effect of hemodynamic variability on Granger causality analysis of fMRI", Neuroimage, 52, 884-96, 2010.

[16] K.J. Friston, L. Harrison, W. Penny, "Dynamic causal modelling", Neuroimage, 19, 1273-1302, 2003.

[17] C. Andrieu, A. Doucet, R. Holenstein, "Particle Markov chain Monte Carlo methods," Journal of the Royal Statistical Society, 72(3), 269-302, 2010.

[18] C. J. Geyer, "Introduction to Markov chain Monte Carlo," in S. Brooks, A. Gelman, G. Jones, X. Meng (Eds.), Handbook of Markov chain Monte Carlo, CRC Press, Taylor and Francis Group, 2011.

[19] M.F. Ahmad, J. Murphy, D. Vatansever, E.A. Stamatakis, S. Godsill, "Tracking changes in functional connectivity of brain networks from resting-state fMRI using Particle Filters," IEEE International Conference on Acoustics, Speech and Signal Processing, 2015.

[20] S. Ancherbak, E.E. Kuruoğlu, M. Vingron, "Time-dependent Gene Network Modeling by Sequential Monte Carlo," IEEE/ACM Transactions on Bioinformatics and Computational Biology, 13, 1183-1193, 2016.

[21] P.M. Djuric, J.H. Kotecha, J. Zhang, Y. Huang, T. Ghirmai , M.F. Bugallo, J. Miguez, "Particle Filtering," IEEE Signal Processing Magazine, 20, 19-38, 2003.

[22] M.S. Arulampalam, S. Maskell, N. Gordon, T. Clapp, "A tutorial on particle filters for nonlinear/non-gaussian bayesian tracking," IEEE Transactions on Signal Processing, 50, 174-188, 2002.

[23] M. Costagli, E.E. Kuruoğlu, "Image separation using particle filters," Digital Signal Processing, 17, 935–946, 2007.

[24] P.A. Valdés-Sosa, A. Roebroeck, J. Danizeau, K. Friston, "Effective connectivity: influence, causality and biophysical modeling," Neuroimage, 58, 339-61, 2011.

[25] A. Gaglianese, M. Costagli, G. Bernardi, E. Ricciardi, P. Pietrini, "Evidence of a direct influence between the thalamus and hMT+ independent of V1 in the human brain as measured by fMRI," Neuroimage , vol. 60 (pg. 1440-7), 2012.

[26] J. Casorso, X. Kong, W. Chi, D. Van De Ville c,d, B.T. T. Yeo, R. Liègeois, "Dynamic mode decomposition of resting-state and task fMRI", Neuroimage, 194, 42-54, 2019.

[27] A. Doucet, S. Godsill, C. Andrieu, "On sequential Monte Carlo sampling methods for Bayesian filtering," Statistics and Computing, 10, 197-208, 2000.

[28] J.S. Liu, R. Chen, "Blind Deconvolution via Sequential Imputations," Journal of the American Statistical Association, 90, 567-576, 1995.

[29] L. Murray, A.J. Storkey, "Continuous time particle filtering for fMRI," Advances in Neural Information Processing Systems (NIPS), 1049-1056, 2008.

[30] R. B. Buxton, E. C. Wong, L. R. Frank, "Dynamics of blood flow and oxygenation changes during brain activation: The balloon model," Magnetic Resonance in Medicine, 39(6), 855-864, 1998.

[31] M.F. Ahmad, J. Murphy, D. Vatansever, E.A. Stamatakis, S. Godsill, "Bayesian inference of task-based functional brain connectivity using Markov chain Monte Carlo methods," IEEE Journal of Selected Topics in Signal Processing, 10(7), 1150-1159, 2016.

[32] G.K. Aguirre, E. Zarahn, et al., "Empirical analyses of BOLD fMRI statistics: II. Spatially smoothed data collected under null-hypothesis and experimental conditions", NeuroImage 5 (3), 199– 212, 1997.

[33] D.A. Handwerker, J.O. Ollinger, M. D'Esposito, "Variation of BOLD hemodynamic responses across subjects and brain regions and their effects on statistical analyses", Neuroimage, 21, 1639-51, 2004.

[34] A. Duggento, L.Passamonti, G. Valenza, R. Barbieri, M. Guerrisi, N. Toschi, "Multivariate Granger causality unveils directed parietal to prefrontal cortex connectivity during task-free MRI", Scientific Report, 8, 1–11, (2018).